

# Polyoxometalate-Derived Ir/WO<sub>x</sub>/rGO Nanocomposites for Enhanced Electrocatalytic Water Splitting

Bo Huang<sup>ID</sup>, Yuntian Ma, Zhelun Xiong, Zicheng Xiao\*, Pingfan Wu\*, Peng Jiang\*, and Minghui Liang\*

**Iridium (Ir)-based nanomaterials are promising electrocatalysts for water splitting, and to alleviate their costs as well as improve the performances are always important tasks. Polyoxometalates (POMs) composed of abundant metal, oxygen, and heteroatoms are nanoclusters with defined structures. Benefitting from the inherent advantages of POMs, highly dispersive and “unprotected” Ir nanoparticles originating from Ir-based colloid solution were successfully anchored on POM-derived WO<sub>3</sub>/rGO nanocomposites for the first time. Interestingly, the obtained hybrid material Ir/WO<sub>x</sub>/rGO delivered improved electrocatalytic performance for water splitting, which is attributed to the addition of only quite small amount of POM derivatives. This work is also the first proof that POM can be employed as precursor to construct metal oxides to support Ir catalysts, providing a new vision for the design of advanced multi-metal electrocatalysts.**

Electrocatalytic water splitting is one of the most promising pathways for energy conversion because the raw material is quite abundant and clean.<sup>[1]</sup> A major difficulty in such electrochemical reactions including hydrogen evolution reaction (HER) and oxygen evolution reaction (OER) is the high overpotentials on account of their sluggish kinetics.<sup>[2]</sup> To develop iridium (Ir)-based electrocatalysts is a promising solution for this problem because they possess suitable binding energy for the adsorption and desorption of catalytic intermediates from water.<sup>[3–5]</sup> However, the large-scale application of such catalysts is limited by their high prices. Hence, it is an urgent task to reduce the cost and further improve the efficiency of Ir-based electrocatalysts. Three fundamental directions are always adopted to face the above issues at present: firstly, reduce the sizes of Ir-based electrocatalysts to nanoscale

or even single-atom scale by regulating their morphology to improve the atomic utilization;<sup>[6–8]</sup> secondly, find suitable catalyst supports to improve their electrochemical performance and stability;<sup>[9–11]</sup> finally, enhance their catalytic activities by adding co-catalysts or forming alloys with abundant metals.<sup>[12–16]</sup> For example, some recent reports have demonstrated that the electrocatalytic performance of Ir-based catalysts can be remarkably enhanced after doping with semiconductive metal oxides such as TiO<sub>2</sub>.<sup>[17,18]</sup>

Tungsten trioxide (WO<sub>3</sub>) has been widely applied as an excellent support and promoter for the noble metal catalyst due to its low price, tuneable composition, good thermal, and chemical stability.<sup>[19]</sup> There have been several reports that WO<sub>3</sub> can enhance the catalytic per-

formance of Pt or Pd catalysts for methanol oxidation and water splitting.<sup>[20–22]</sup> WO<sub>3</sub> is also a promising candidate of electrode materials for water splitting which may show excellent performance and stability in both HER and OER by suitably tailoring its geometric and electronic structure.<sup>[23,24]</sup> However, the combination of Ir and WO<sub>3</sub> has been rarely reported,<sup>[25,26]</sup> and Ir/WO<sub>3</sub> catalysts have not been applied to electrocatalytic water splitting yet. This is mainly because that the synthesis of such nanocomposites still faces the problems such as uncontrollable preparation and irregular dispersion, which still need to be overcome.

Polyoxometalates (POMs) are nanoclusters composed of abundant transition metals, oxygen atoms, and heteroatoms.<sup>[27]</sup> Recent reports indicate that POMs are excellent precursors to prepare well dispersed, nanoscale, and porous metal composites (such as metal oxides and carbides) by carbonization.<sup>[28–30]</sup> Interestingly, these composites can be employed as electrode materials with outstanding electrochemical performance in rechargeable batteries and electrocatalytic water splitting.<sup>[31–33]</sup> Such advantages can be attributed to the unique structural features of POM precursors: the defined molecular structure and layer-by-layer crystal packing of POMs can prevent the agglomeration during the heating process; the abundant oxygen atoms in POM clusters can facilitate the carbonization between POMs and carbon sources, which can produce porous architectures during oxycarbides release and further improve the diffusion of electrolytes, ions, and electrons.<sup>[34–37]</sup> These nanocomposites can also be applied as supports and co-catalyst for noble metal catalysts with enhanced catalytic performance by synergistic effect.<sup>[38]</sup>

Considering the three fundamental directions to design advanced Ir-based electrocatalysts, in this communication, we successfully prepared

B. Huang, Y. Ma, Z. Xiong, Prof. P. Jiang, Prof. M. Liang  
CAS Center for Excellence in Nanoscience, CAS Key Laboratory of  
Nanosystem and Hierarchical Fabrication, CAS Key Lab Standardization &  
Measurement Nanotechnology, National Center for Nanoscience and  
Technology, Beijing 100190, China

E-mail: pjiang@nanoctr.cn

E-mail: liangmh@nanoctr.cn

B. Huang, Prof. Z. Xiao, Prof. P. Wu

Institute of POM-based Materials, Hubei University of Technology, Wuhan  
430068, China

E-mail: zichengxiao@hotmail.com

E-mail: pingfanwu-111@163.com

B. Huang, Prof. P. Jiang

University of Chinese Academy of Sciences, Beijing 100049, China

<sup>ID</sup> The ORCID identification number(s) for the author(s) of this article  
can be found under <https://doi.org/10.1002/eeem.2.12150>.

DOI: 10.1002/eeem.2.12150

Ir/WO<sub>3</sub>/rGO nanocomposites originating from Ir colloid solution and POM precursor for the first time. A Keggin-type POM H<sub>3</sub>O<sub>40</sub>PW<sub>12</sub> (PW<sub>12</sub>) was applied as a precursor to obtain nanosized and well-dispersed WO<sub>3</sub> on graphene supports. The “unprotected” Ir nanoparticles (NPs) with uniform size distribution and high atomic utilization were prepared using metal-based colloid solution<sup>[39–42]</sup> and were successfully decorated onto the WO<sub>3</sub>/rGO surface. This tri-component catalyst showed enhanced electrochemical performance for HER, OER, and overall water splitting in 1 M KOH, which can be seemed as one of most promising electrocatalysts. Such procedure also opens a new mind for the design of advanced electrocatalysts via colloid and POM precursors.

The Ir/WO<sub>3</sub>/rGO was prepared via the following procedure (**Scheme 1**): Firstly, PW<sub>12</sub> was loaded on the GO surfaces by mixing its aqueous solution with GO dispersion. Then, the mixture was dried and carbonized at 800°C under Ar atmosphere. PW<sub>12</sub> was collapsed to form WO<sub>3</sub> NPs and successfully anchored on the graphene (WO<sub>3</sub>/rGO). Finally, Ir colloid solution (0.21 wt%), which was prepared according to our previous report,<sup>[39]</sup> was mixed with the WO<sub>3</sub>/rGO to form the aimed Ir/WO<sub>3</sub>/rGO nanocomposites. The contents of Ir and W are 4.33 wt% and 0.36 wt% (ICP-OES). As comparison, Ir/rGO and WO<sub>3</sub>/rGO were also prepared by the similar procedure (commercial chemists are listed in Table S1 and detailed experimental section is also shown in Supplementary Information).

The structural and morphology features of the nanocomposites were investigated by SEM, TEM, and XRD techniques. SEM results indicate that the morphology of graphene nanosheets can be maintained after stepwise functionalization, and there is no apparent agglomeration between these nanosheets (Figure S1–S2). TEM images of WO<sub>3</sub>/rGO display clear facets with lattice fringes of WO<sub>3</sub> in the sized of approximately 5 nm (**Figure 1a–b**). The XRD pattern of the WO<sub>3</sub>/rGO also shows obvious feature peaks of WO<sub>3</sub> (PDF#33-1387) (**Figure S3**). These results demonstrate that the WO<sub>3</sub> NPs are successfully loaded on the rGO surfaces.

TEM images of Ir/WO<sub>3</sub>/rGO show Ir NPs with the sized of 1–2 nm (**Figure 1c–e**), which is in accord with the Ir NPs in solution.<sup>[43]</sup> The lattice fringes on the surface were also in consistence with the Ir(111) plane. The STEM and elemental mapping results show that the mixed metals (Ir and W) and heteroatom (P) are well dispersed on the surface of graphene nanosheets, giving a concrete evidence that the Ir NPs are successfully loaded on the WO<sub>3</sub>/rGO (**Figure 1f**). In addition, the Ir/WO<sub>3</sub>/rGO still shows clear WO<sub>3</sub> peaks in XRD result but with a little shift compared to that of WO<sub>3</sub>/rGO. This is because WO<sub>3</sub> nanoparticles are partly reduced by the Ir colloid solution (inherent glycol/alkaline solvent) during the loading procedure so that part of oxygen atoms is released from the surface and the reduced tungsten atoms are inserted into the lattice.

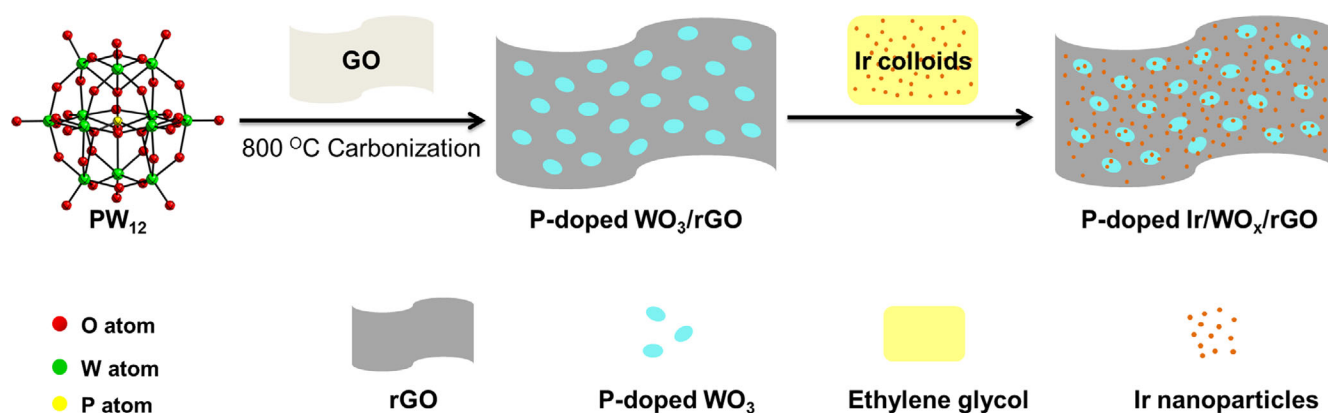
XPS was applied to investigate the surface compositions and chemical states of these new nanocomposites (**Figure S4**). The high-resolution spectra of Ir4f can be well fitted into two peaks, and the binding energies of Ir4f<sub>7/2</sub> for Ir/rGO and Ir/WO<sub>3</sub>/rGO are 62.0 eV and 62.1 eV, respectively. This result indicates that Ir NPs remain metallic state after anchored on the surface of rGO or WO<sub>3</sub>/rGO composites. On the other hand, the high-resolution spectra of W4f of WO<sub>3</sub>/rGO can be fitted into two peaks including W4f<sub>7/2</sub> (35.8 eV) and W4f<sub>5/2</sub> (37.9 eV), revealing the W<sup>6+</sup> oxidation state in WO<sub>3</sub>/rGO composite. After Ir NPs loaded onto the surface of WO<sub>3</sub>/rGO, the high-resolution spectra of W4f can be divided into two categories including W<sup>6+</sup> and W<sup>0</sup> for Ir/WO<sub>3</sub>/rGO hybrid material. The binding energy of W<sup>0</sup>4f<sub>7/2</sub> is 33.0 eV, indicating that parts of the W<sup>6+</sup> were reduced to metallic

state after Ir NPs loaded onto the surface of WO<sub>3</sub>/rGO. This phenomenon keeps consistence with the previous study of IrW nanobranes<sup>[44]</sup> and IrW nanodendrites,<sup>[45]</sup> and is also accord with the above XRD results.

The electrocatalytic performances of these nanocomposites have been explored in alkaline condition (1 M KOH). Linear sweep voltammetry (LSV) was firstly applied to measure the overpotentials toward HER. As shown in **Figure 2a**, the overpotentials of Ir/rGO and Ir/WO<sub>3</sub>/rGO at current density of 10 mA cm<sup>−2</sup> ( $\eta_{10}$ ) are 92 and 53 mV, respectively. On the other hand, WO<sub>3</sub>/rGO shows bad electrocatalytic activities for HER. This result indicates that the electrocatalytic performance of Ir NPs is effectively improved after loading onto WO<sub>3</sub>/rGO surface and the  $\eta_{10}$  value of Ir/WO<sub>3</sub>/rGO is even closed to commercial Pt/C catalyst as well as reported results (Table S2). The Tafel slopes were measured to evaluate the electrocatalytic kinetics of these electrocatalysts (**Figure 2b**). The Tafel slope of Ir/WO<sub>3</sub>/rGO is 43 mV dec<sup>−1</sup>, thus, the mechanism of the HER reaction follows through the Volmer – Heyrovsky reaction and the rate-determining step is the Heyrovsky step. In addition, the Tafel slope of the HER reaction with Ir/WO<sub>3</sub>/rGO catalyst is closed to the characteristic slope of Heyrovsky step in low overpotential area, indicating that Ir/WO<sub>3</sub>/rGO has a rapid kinetics process for HER. According to the previous reports,<sup>[44,45]</sup> a plausible explanation for the enhanced performance of Ir/WO<sub>3</sub>/rGO is that Ir formed alloy with W on the surface of the WO<sub>3</sub> NPs, which can be observed from the XPS spectra. As mentioned above, the HER followed a two-stage process which is known as Volmer and Heyrovsky reaction. A key factor for the both two reactions is the dissociation of water molecules on the surface of catalyst. W atom has a stronger binding energy for the dissociated OH\* than Ir. The strong affinity of the surface W site to OH\* can lower the free energy of the Volmer and Heyrovsky steps, and reduce the barrier of HER in alkaline solution. On the other hand, previous reports indicate that the electrocatalytic performance can be enhanced through the alloyed interfaces between metals and WO<sub>3</sub> nanoparticles, such as Pt/WO<sub>3</sub> for methanol oxidation,<sup>[21]</sup> Pd/WO<sub>3</sub> for zinc – air batteries,<sup>[22]</sup> and Mn- or V- doped WO<sub>3</sub> for water splitting.<sup>[23]</sup> Hence, the improved performance of Ir/WO<sub>3</sub>/rGO for water splitting is owing to the interaction between Ir and WO<sub>3</sub>.

The OER performances of these electrocatalysts were also explored (**Figure 2c,d**). The overpotentials of Ir/rGO and Ir/WO<sub>3</sub>/rGO at  $\eta_{10}$  are 444 and 265 mV, respectively. It is fascinating that Ir/WO<sub>3</sub>/rGO can deliver much better electrocatalytic performance than that of Ir/rGO, and even significantly better than the commercial IrO<sub>2</sub> benchmark (294 mV). As WO<sub>3</sub>/rGO shows little electrocatalytic activities for OER, it can be concluded that WO<sub>3</sub> can also improve the electrocatalytic OER performance of Ir NPs. As a consequence, the ultralow overpotential of Ir/WO<sub>3</sub>/rGO is even more outstanding than most of the previous reports (Table S3).<sup>[46–48]</sup>

The electrochemical surface areas (ECSA) of these electrocatalysts were evaluated through measuring their electrochemical double-layer capacitance value ( $C_{dl}$ ) by CV method at different scan rates (**Figure S5**). Ir/WO<sub>3</sub>/rGO possesses a higher ECSA value of 10.2 mF cm<sup>−2</sup> than that of Ir/rGO (3.6 mF cm<sup>−2</sup>). Hence, the interaction between electrolyte and the surface of electrocatalysts for Ir/WO<sub>3</sub>/rGO is much beneficial, and the diffusion of ions can be enhanced. This is also one of the reasons why Ir/WO<sub>3</sub>/rGO delivers the best electrocatalytic performance. On the other hand, electrochemical impedance spectroscopy (EIS) was applied to further study these electrocatalysts (**Figure S6**). Ir/WO<sub>3</sub>/rGO exhibits a lowest charge transfer resistance ( $R_{ct}$ ) value (18.5  $\Omega$ ) at overpotential of 200 mV, indicating that Ir/WO<sub>3</sub>/rGO possesses



**Scheme 1.** Synthetic scheme of P-doped Ir/WO<sub>x</sub>/rGO nanocomposite originating from Ir-based colloid solution and POM precursor.

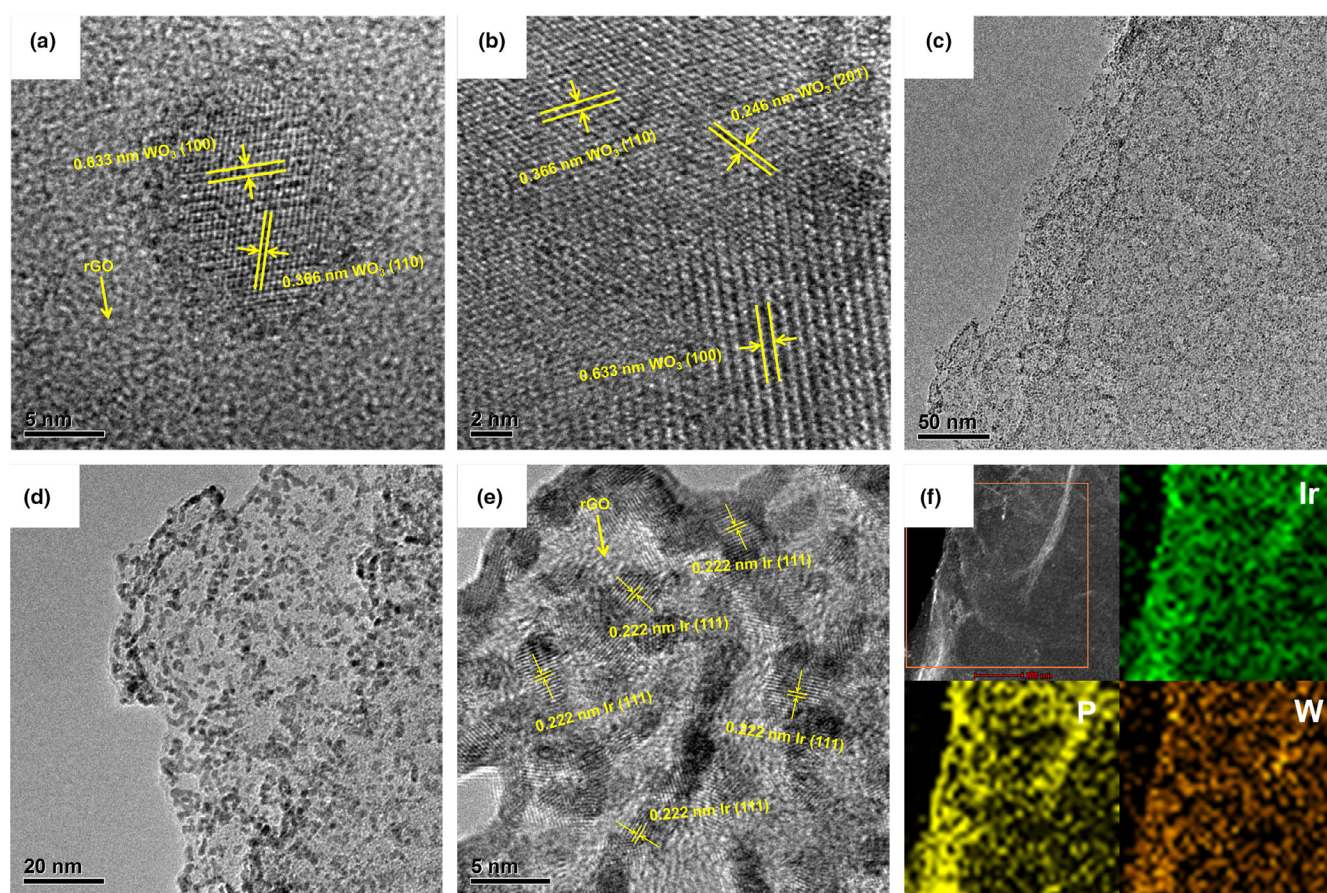


**Figure 1.** a-b) TEM images of WO<sub>3</sub>/rGO and c-e) Ir/WO<sub>x</sub>/rGO; f) STEM image and elemental mapping of Ir/WO<sub>x</sub>/rGO.

the fastest electron transfer rate. Thus, Ir/WO<sub>x</sub>/rGO can deliver the lowest overpotential for electrocatalytic reactions.

The durability of Ir/WO<sub>x</sub>/rGO was further investigated after ultra-long HER cycles (Figure 2e). The overpotential at  $\eta_{10}$  can be maintained at 55 mV after 10 000 cycles and at 59 mV after further consecutive 12 h chronoamperometry. There is no apparent change compared with its initial overpotential at  $\eta_{10}$  (53 mV). The durability

test of such electrocatalyst in OER is shown in Figure 2f. The overpotential of Ir/WO<sub>x</sub>/rGO at  $\eta_{10}$  can be maintained at 283 mV after 10 000 cycles and at 292 mV after further consecutive 12 h chronoamperometry. In addition, XPS and XRD results indicate that the initial structure of the electrocatalyst was well maintained after the durability tests (Figure S7). The morphologies of the nanocomposite revealed SEM (including EDS) studies also show no obvious agglomeration after

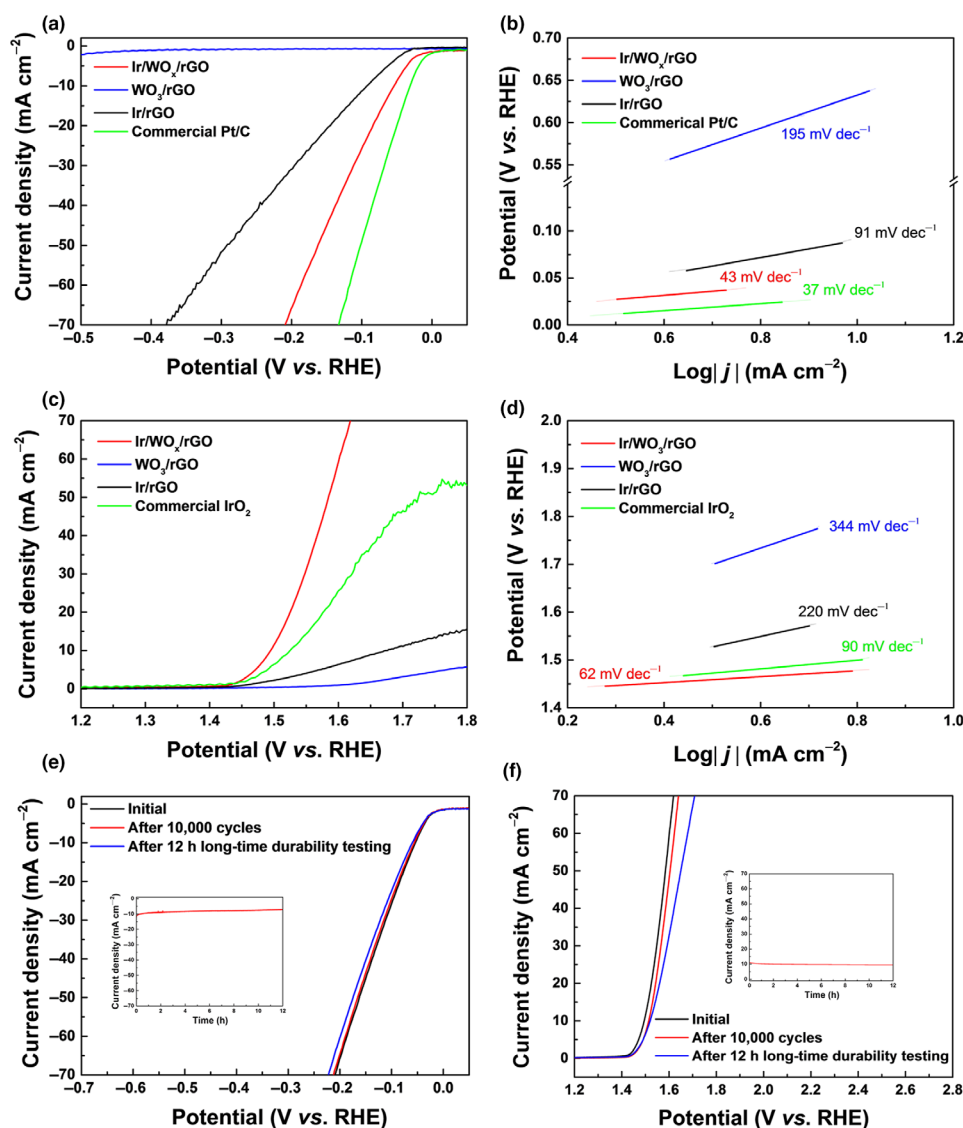


**Figure 2.** a-b) LSV curves and Tafel slopes of the electrocatalysts for HER and c-d) OER, respectively; Cycling performance after long-time durability testing of Ir/WO<sub>x</sub>/rGO for e) HER and f) OER, respectively.

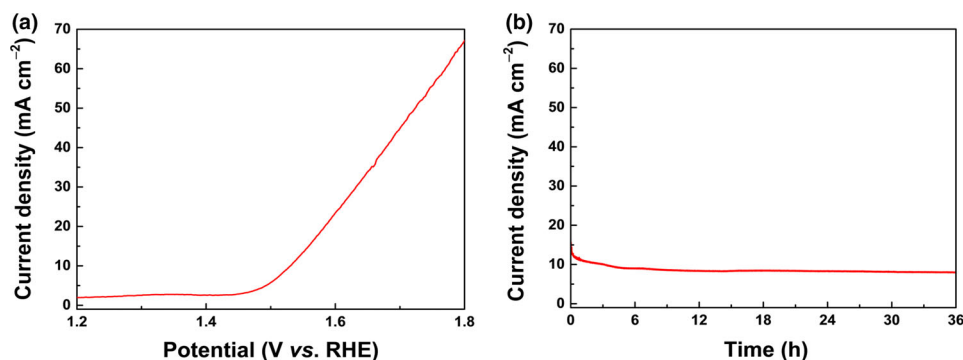


**Figure 3.** a) Overall water splitting performance of Ir/WO<sub>x</sub>/rGO and b) the long-time durability testing for 36h.

ultralong cycles (Figure S8), demonstrating that Ir/WO<sub>x</sub>/rGO is a quite stable electrocatalyst for both HER and OER.

Considering the excellent performance in both HER and OER, Ir/WO<sub>x</sub>/rGO modified electrodes were applied as both cathode and anode for overall water splitting. The LSV curve (Figure 3a) shows the outstanding performance that only 1.53 V is needed at  $\eta_{10}$ . In addition, the Ir/WO<sub>x</sub>/rGO electrodes can maintain the current density after consecutively working for 36h, indicating that such electrode material has a prominent electrochemical stability (Figure 3b). This result is much better than the previous reports of Ir/W electrocatalysts by involving IrCl<sub>3</sub> and W(CO)<sub>6</sub> as the metal precursors,<sup>[44,45]</sup> and even better than most of literatures (Table S4). The improved performance of such novel nanocomposite can be owing to the benefits from the synthetic procedure: 1) POMs have specific structures with inherent abundant metal atoms, oxygen atoms, and heteroatoms; hence, no additional metal or heteroatom source is needed; 2) oxygen atoms in POMs can be released by carbonization and produce hierarchical architectures in the derivatives; 3) the Ir NPs from colloidal solution are “unprotected” and the surfaces of the NPs are completely exposed; 4) there are no additional wrapped chemicals such as organic polymers; 5) such Ir NPs are narrow size distribution and not inclined to aggregate. Thus, the derived Ir/WO<sub>x</sub>/rGO can show outstanding electrocatalytic performance.

In conclusion, Ir-based colloidal solution and POM clusters are employed to fabricate multi-metal electrocatalysts for the first time. This is also the first attempt to design Ir/WO<sub>x</sub>/rGO nanocomposites and to explore their electrocatalytic performance for water splitting. The combination of Ir and POM derivative can enhance the electrocatalytic performance and durability for both HER and OER. The overpotentials at  $\eta_{10}$  are 53 mV and 265 mV for HER and OER, respectively. Their performances are extremely improved than that of Ir/rGO, indicating the small amount

of POM-derived oxide possesses much benefit to the electrocatalytic property of Ir-based catalysts. The nanocomposite also has an outstanding performance for overall water splitting and only 1.53 V is needed at  $\eta_{10}$ , which is much better than most of the reported electrocatalysts. In addition, the novel electrocatalyst can maintain its low overpotentials after ultralong cycling tests for HER, OER, and overall water splitting, exhibiting excellent electrocatalytic stability. Hence, this work not only provides a novel alternative Ir-based multifunctional electrocatalysts, but also opens a new mind for the design of advanced functional materials originating from colloids and POM precursors.

## Acknowledgements

This work was supported by Beijing Municipal Science and Technology Project (No. Z161100001116080), Cross training plan for high level talents in Beijing colleges and university, Major Project of the Ministry of Science and Technology (No. 2016YFA0200904, 2016YFC0600605), Chinese Academy of Geological Sciences Fundamental Research projects (No. YYWF201619), Comprehensive geological survey of Yunnan Anning Mine Concentration Zone (No. DD20190589), National Natural Science Foundation of China (No. 21271068, 21401050), the Natural Science Foundation of Hubei Province (No. 2015CFA131), and Wuhan Applied Basic Research Program (No. 2014010101010020). B. H., Z. X., P. W., P. J., and M. L. provided the idea of this work. B. Huang, Z. X., and P. W. designed the precursor of polyoxometalate. B. H., P. J., and M. L. conducted the electrocatalytic tests and analyzed the results. The experiments were conducted by B. H., and the characterizations were performed by B. H., Y. M., and Z. X. All authors organized this manuscript. Z. X., P. W., P. J., and M. L. provided the research funding.

## Conflict of Interest

The authors indicate that there is no conflict of interest.

## Supporting Information

Supporting Information is available from the Wiley Online Library or from the author.

## Keywords

polyoxometalates, iridium, electrocatalyst, water splitting

Received: June 26, 2020  
Revised: September 20, 2020  
Published online: October 21, 2020

- [1] Q. Zhang, E. Uchaker, S. L. Candelaria, G. Cao, *Chem. Soc. Rev.* **2013**, 42, 3127.
- [2] A. Eftekhari, *Int. J. Hydrogen Energy* **2017**, 42, 11053.
- [3] L. Fu, P. Cai, G. Cheng, W. Luo, *Sustain. Energy Fuels* **2017**, 1, 1199.
- [4] I. Ali, K. AlGhamdi, F. T. Al-Wadaani, *J. Mol. Liq.* **2019**, 280, 274.
- [5] C. S. Lim, Z. Sofer, R. J. Toh, A. Y. S. Eng, J. Luxa, M. Pumera, *ChemPhysChem* **1898**, 2015, 16.
- [6] Y. Peng, B. Lu, S. Chen, *Adv. Mater.* **2018**, 30, e1801995.
- [7] Q. Wang, M. Ming, S. Niu, Y. Zhang, G. Fan, J. S. Hu, *Adv. Energy Mater.* **2018**, 8, 1801698.
- [8] P. Lettenmeier, J. Majchel, L. Wang, V. A. Saveleva, S. Zafeiratos, E. R. Savinova, J. J. Gallet, F. Bournel, A. S. Gago, K. A. Friedrich, *Chem. Sci.* **2018**, 9, 3570.

- [9] K. Choi, S. Lee, Y. Shim, J. Oh, S. Kim, S. Park, *2d Mater.* **2015**, 2, 34019.
- [10] A. Epshteyn, Y. Garsany, K. L. More, H. M. Meyer, V. Jain, A. P. Purdy, K. E. Swider-Lyons, *ACS Catal.* **2015**, 5, 3662.
- [11] V. Perazzolo, C. Durante, R. Pilot, A. Paduano, J. Zheng, G. A. Rizzi, A. Martucci, G. Granozzi, A. Gennaro, *Carbon* **2015**, 95, 949.
- [12] P. Jiang, J. Chen, C. Wang, K. Yang, S. Gong, S. Liu, Z. Lin, M. Li, G. Xia, Y. Yang, J. Su, Q. Chen, *Adv. Mater.* **2018**, 30, 1705324.
- [13] J. Feng, F. Lv, W. Zhang, P. Li, K. Wang, C. Yang, B. Wang, Y. Yang, J. Zhou, F. Lin, G. C. Wang, S. Guo, *Adv. Mater.* **2017**, 29, 1703798.
- [14] X. Wang, Q. Kong, Y. Han, Y. Tang, X. Wang, X. Huang, T. Lu, *J. Electroanal. Chem.* **2019**, 838, 101.
- [15] Q. Shi, C. Zhu, D. Du, J. Wang, H. Xia, M. H. Engelhard, S. Feng, Y. Lin, *J. Mater. Chem. A* **2018**, 6, 8855.
- [16] D. Liu, S. Lu, Y. Xue, Z. Guan, J. Fang, W. Zhu, Z. Zhuang, *Nano Energy* **2019**, 59, 26.
- [17] C. Wang, F. Lan, Z. He, X. Xie, Y. Zhao, H. Hou, L. Guo, V. Murugadoss, H. Liu, Q. Shao, Q. Gao, T. Ding, R. Wei, Z. Guo, *Chemsuschem* **2019**, 12, 1576.
- [18] M. Bernicke, D. Bernsmeier, B. Paul, R. Schmack, A. Bergmann, P. Strasser, E. Ortel, R. Kraehnert, *J. Catal.* **2019**, 376, 209.
- [19] G. Zheng, J. Wang, H. Liu, V. Murugadoss, G. Zu, H. Che, C. Lai, H. Li, T. Ding, Q. Gao, Z. Guo, *Nanoscale* **2019**, 11, 18968.
- [20] W. Wu, X. D. Xiang, Y. L. Lin, W. S. Li, *Int. J. Hydrogen Energy* **2013**, 38, 11080.
- [21] T. Tsurumura, N. Yoshimoto, M. Egashira, M. Morita, *Electrochemistry* **2012**, 80, 916.
- [22] R. Choudhary, S. Patra, R. Madhuri, P. K. Sharma, A. C. S. Sustain, *Chem. & Eng.* **2017**, 5, 9735.
- [23] S. Chandrasekaran, P. Zhang, F. Peng, C. Bowen, J. Huo, L. Deng, *J. Mater. Chem. A* **2019**, 7, 6161.
- [24] T. Zheng, W. Sang, Z. He, Q. Wei, B. Chen, H. Li, C. Cao, R. Huang, X. Yan, B. Pan, S. Zhou, J. Zeng, *Nano Lett.* **2017**, 17, 7968.
- [25] M. Dhanalakshmi, S. Lakshmi Prabavathi, K. Saravanakumar, B. Filip Jones, V. Muthuraj, *Chem. Phys. Lett.* **2020**, 745, 137285.
- [26] M. Bastuck, D. Puglisi, J. Huotari, T. Sauerwald, J. Lappalainen, A. Lloyd Spetz, M. Andersson, A. Schütze, *Thin Solid Films* **2016**, 618, 263.
- [27] E. Coronado, C. J. Gomez-Garcia, *Chem. Rev.* **1998**, 98, 273.
- [28] Y. Ji, L. Huang, J. Hu, C. Streb, Y. F. Song, *Energy & Environ. Sci.* **2015**, 8, 776.
- [29] D. Zhou, Y. Cui, P. W. Xiao, M. Y. Jiang, B. H. Han, *Nature Commun.* **2014**, 5, 4716.
- [30] Y. J. Tang, M. R. Gao, C. H. Liu, S. L. Li, H. L. Jiang, Y. Q. Lan, M. Han, S. H. Yu, *Angew. Chem. Int. Ed.* **2015**, 54, 12928.
- [31] B. Huang, D. H. Yang, B. H. Han, *J. Mater. Chem. A* **2020**, 8, 4593.
- [32] Y. Huang, J. Ge, J. Hu, J. Zhang, J. Hao, Y. Wei, *Adv. Energy Mater.* **2018**, 8, 1701601.
- [33] Y. Huang, Y. Sun, X. Zheng, T. Aoki, B. Pattengale, J. Huang, X. He, W. Bian, S. Younan, N. Williams, J. Hu, J. Ge, N. Pu, X. Yan, X. Pan, L. Zhang, Y. Wei, J. Gu, *Nature Commun.* **2019**, 10, 982.
- [34] F. Yu, Y. Gao, Z. Lang, Y. Ma, L. Yin, J. Du, H. Tan, Y. Wang, Y. Li, *Nanoscale* **2018**, 10, 6080.
- [35] H. Yan, Y. Xie, Y. Jiao, A. Wu, C. Tian, X. Zhang, L. Wang, H. Fu, *Adv. Mater.* **2018**, 30, 1704156.
- [36] H. Wei, Q. Xi, X. Chen, D. Guo, F. Ding, Z. Yang, S. Wang, J. Li, S. Huang, *Adv. Sci.* **2018**, 5, 1700733.
- [37] J. Ge, J. Hu, Y. Zhu, O. Zeb, D. Zang, Z. Qin, Y. Huang, J. Zhang, Y. Wei, *Acta Phys-Chim. Sin.* **2020**, 36, 1906063.
- [38] H. Yan, C. Tian, L. Sun, B. Wang, L. Wang, J. Yin, A. Wu, H. Fu, *Energy Environ. Sci.* **2014**, 7, 1939–49.
- [39] I. Schrader, J. Warneke, S. Neumann, S. Grotheer, A. A. Swane, J. J. K. Kirkensgaard, M. Arenz, S. Kunz, *J. Phys. Chem. C* **2015**, 119, 17655.
- [40] J. Quinson, M. Inaba, S. Neumann, A. A. Swane, J. Bucher, S. B. Simonsen, L. Theil Kuhn, J. J. K. Kirkensgaard, K. M. Ø. Jensen, M. Oezaslan, S. Kunz, M. Arenz, *ACS Catal.* **2018**, 8, 6627.
- [41] J. Quinson, J. Bucher, S. B. Simonsen, L. T. Kuhn, S. Kunz, M. Arenz, A. C. S. Sustain, *Chem. & Eng.* **2019**, 7, 13680.

- [42] Y. Wang, J. Zhang, X. Wang, J. Ren, B. Zuo, Y. Tang, *Top. Catal.* **2005**, 35, 35.
- [43] B. Huang, Y. Ma, Z. Xiong, W. Lu, R. Ding, T. Li, P. Jiang, M. Liang, *Sustain. Energy Fuels*. **2020**, 4, 2388.
- [44] F. Lv, J. Feng, K. Wang, Z. Dou, W. Zhang, J. Zhou, C. Yang, M. Luo, Y. Yang, Y. Li, P. Gao, S. Guo, *ACS Cent Sci.* **2018**, 4, 1244.
- [45] L. Fu, X. Hu, Y. Li, G. Cheng, W. Luo, *Nanoscale* **2019**, 11, 8898.
- [46] X. Zhang, X. Zhang, H. Xu, Z. Wu, H. Wang, Y. Liang, *Adv. Funct. Mater.* **2017**, 27, 1606635.
- [47] M. Gong, W. Zhou, M.-C. Tsai, J. Zhou, M. Guan, M.-C. Lin, B. Zhang, Y. Hu, D.-Y. Wang, J. Yang, S. J. Pennycook, B.-J. Hwang, H. Dai, *Nature Commun.* **2014**, 5, 4695.
- [48] J. Zhang, T. Wang, P. Liu, S. Liu, R. Dong, X. Zhuang, M. Chen, X. Feng, *Energy & Environ. Sci.* **2016**, 9, 2789.